

Three-dimensional geotechnical analysis on a strongly altered sedimentary domain at Bozshakol copper mine

B Adiyansyah KAZ Minerals, Kazakhstan

D Gorokhov KAZ Minerals, Kazakhstan

B Rakhmetov KAZ Minerals, Kazakhstan

J Caratti KAZ Minerals, Kazakhstan

N Bar KAZ Minerals, Kazakhstan

Abstract

Bozshakol is a large open pit copper mine located in north Kazakhstan. During the initial mining phases, a series of multi-bench instabilities developed within a complex, sheared sedimentary rock mass on the south wall of the pit. These were safely managed using prism and radar monitoring.

This paper discusses three-dimensional geotechnical back-analyses that were used alongside information obtained from a series of geotechnical investigation programs and laboratory testing to determine realistic shear strength parameters for the complex materials in the geotechnical model. With improved geotechnical model confidence, forward analysis was completed to enable slope optimisation for future pushbacks and to provide guidance on slope depressurisation requirements for key geotechnical domains.

Keywords: *anisotropy, limit equilibrium analysis, finite element analysis, 3D slope stability model, slope stability radar*

1 Introduction

The Bozshakol deposit is large-scale open pit mine located in the Ekibastuz district of the Pavlodar region in the Republic of Kazakhstan. The mine is situated approximately 250 km east of Astana and 230 km northeast of Karaganda. The topography of the area surrounding the mine is dominated by gently undulating hills and small ridges approximately 15–20 m high. These create numerous small, closed surface runoff catchments and lakes (AMC Consultants Pty Ltd 2010).

The current mining operation is approximately 200 m deep, 4.5 km long in the northeast to southwest orientation and 1.8 km wide in the northwest to southeast orientation. Future pit slope heights are expected to reach 430 m. An average copper grade of 0.33 % with onsite processing facilities have an annual ore processing capacity of 30 million tonnes and a remaining mine life of around 40 years (KAZ Minerals 2023).

Conveniently, the Bozshakol mine area is topographically very flat. As shown in Figure 1, waste dumps are located to the north of the pit, stockpiles are to the southeast and the tailings storage facility is to the west. The processing plant and other mine infrastructures are located to the south of the pit.

During the early stage of pit development, several instabilities were identified within the sedimentary domain on the south wall. Failure mechanisms were considered complex and involved the combination of rock mass-controlled or step-path failures which were typically influenced by intense alteration on narrowly bedded sediments. As shown in Figure 2, a series of cracks and ductile displacements propagated toward the pit direction above and below the main haulage ramp. Safety risks were managed using a combination of prism monitoring and ground-based radar with alarms and 24/7 response protocols in place.



Figure 1 Layout of Bozshakol mine, Republic of Kazakhstan

Several actions were taken to reduce the extent and magnitude of the displacements and risk to the main haulage ramp. These included unloading at the uppermost elevation, localised buttressing, trim blasting for widening the ramp and offsetting the failed crest by constructing safety bunds.

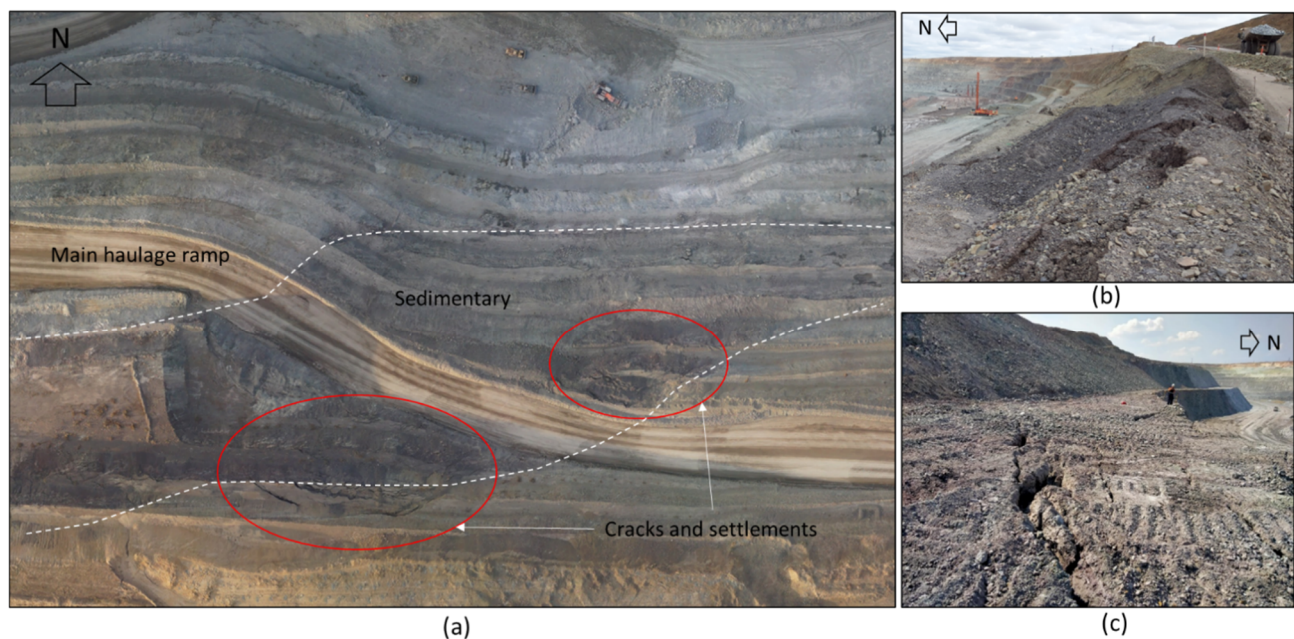


Figure 2 (a) Area of concern at the south wall on the plan view; (b) Lower part looking east; (c) Upper part looking west

The instabilities above and below the main haulage ramp have been effectively controlled using a combination of prism and radar monitoring for early detection and local design adjustments including unloading and buttressing to arrest and/or contain the instabilities. Future pushbacks involving larger slope heights are expected to encounter similar ground conditions within the sedimentary domain. The ground is considered poor, with highly fractured and friable materials found in several areas which have been intensely altered. The bedding planes are quite shallow and dip favourably into the wall. This paper describes

back-analyses undertaken to better understand material strength properties for a more reliable design of the next pushback.

2 Engineering geological setting

2.1 Geology setting

Bozshakol copper mine is located on the western part of the Central Asian Orogenic Belt (Shen et al. 2015). It comprises a Cambrian-Ordovician, high-level intrusive complex emplaced into the east-northeast-trending Bozshakol anticline (Figure 3). Major geological units in the area include Lower-Middle Cambrian sandstones and intermediate-mafic volcanic rocks (lavas and tuffs), unconformably overlaid by Upper Cambrian to Lower Ordovician age mainly clastic sediments. The Lower and Middle Cambrian formations are intruded by granodiorite to tonalite porphyry and porphyritic dykes, which are spatially associated with mineralisation (AMC Consultants Pty Ltd 2010).

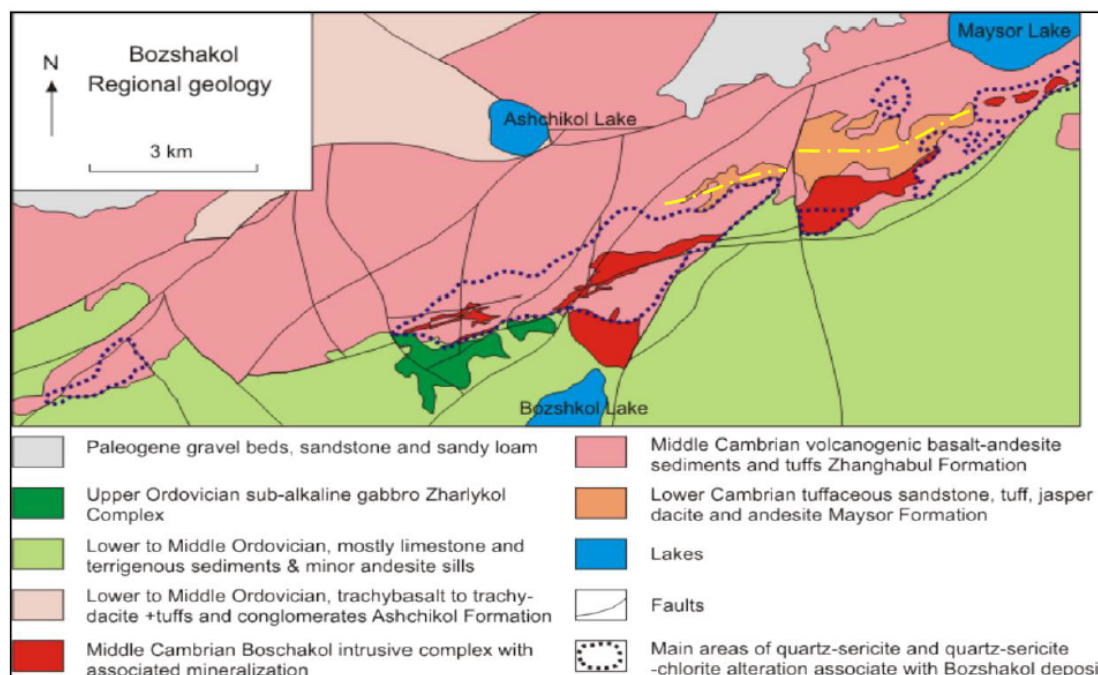
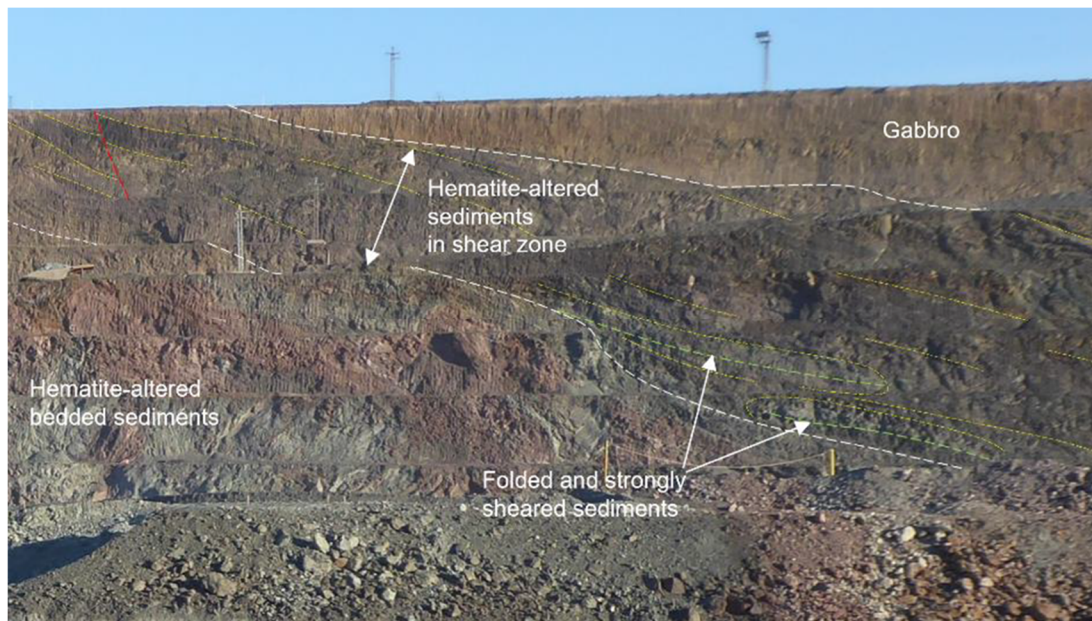


Figure 3 Local geology of the Bozshakol porphyry copper deposit. Yellow dashed line indicates the approximate location of the core of the Bozshakol anticline (after AMC Consultants Pty Ltd 2010)

A major shear zone reaching up to 90 m thick cuts the Lower Ordovician clastic sedimentary succession on the south wall. Within this zone, the bedded sediments are variably deformed and strongly hematite-altered. The Lower Ordovician sedimentary succession that consists of sandstones, siltstones and occasional limestones structurally overlies the volcanics and intrusives that host mineralisation.

The most significant feature within the sediments is a red-brown stained, intensely hematite-altered package of rocks. Within this zone the bedded sediments are moderately to intensely deformed, with beds and laminations attenuated parallel to the margins of the zone. Where deformation is most intense, beds and layers have been strongly sheared. Locally, bedding and laminations define tight folds parallel to the margins of the shear zone on the scale of 10 centimetres to several metres. The hematitic sheared sediments are deformed into folds with steep axial planes, which are believed to partially result from late fault-related deformation. The large-scale shape of the shear zone has a synformal geometry which is likely due to drag and rotation of the shear zone by sinistral displacements on later brittle faults, particularly the main fault zone. Clastic sediments occupying the south pit wall are variably affected by brittle-ductile deformation in a shallow south-dipping shear zone that has been subsequently faulted, folded and locally rotated (Tektonik 2022). Figure 4 shows the appearance of altered sediments observed in the outcrop and core photos.



(a)



(b)

Figure 4 (a) View of the south wall shows hematite-altered sedimentary observed in the outcrop; (b) Photographs of core

2.2 Geotechnical considerations

Geotechnical domains are primarily based on lithology and pit slope sectors. They are further subdivided on the basis of similarities of geotechnical characteristics and, in particular, strength properties on the southern pit wall. Clay domains situated on the uppermost layer underlay by thin saprolite layer before subsequent gabbro domain. Fresh andesite is the dominant host rock and is occasionally intruded by granodiorites. Sedimentary layers between the andesite and gabbro are favourably oriented with bedding orientation dipping into the wall.

Bozshakol represents a very highly-faulted deposit where major structures appear frequently and are interpreted to be interlinked (Tektonik 2022). Two main fault sets can be distinguished:

Northeast–southwest striking faults dominate the current open pit and over the extent of the planned mining area. These faults strike $\sim 020\text{--}070^\circ$ (modal strike = 050°) and dip around $50\text{--}90^\circ$. Approximately 75% of faults in this set dip towards the southeast, predominantly at $60\text{--}75^\circ$. Northwest-dipping faults occur in greater frequency in the southern half of the deposit.

A small number of east–west striking faults are observed principally on the axis of the pit and along the centre of the north wall.

These faults are not wide fault zones and as such are modelled as discrete surfaces. In this particular case study, only northeast–southwest striking faults exist and are taken into account in the analysis. Figure 5 shows a typical section of geotechnical domains including faults and anisotropy surface with the bedding orientation dipping into the slope.

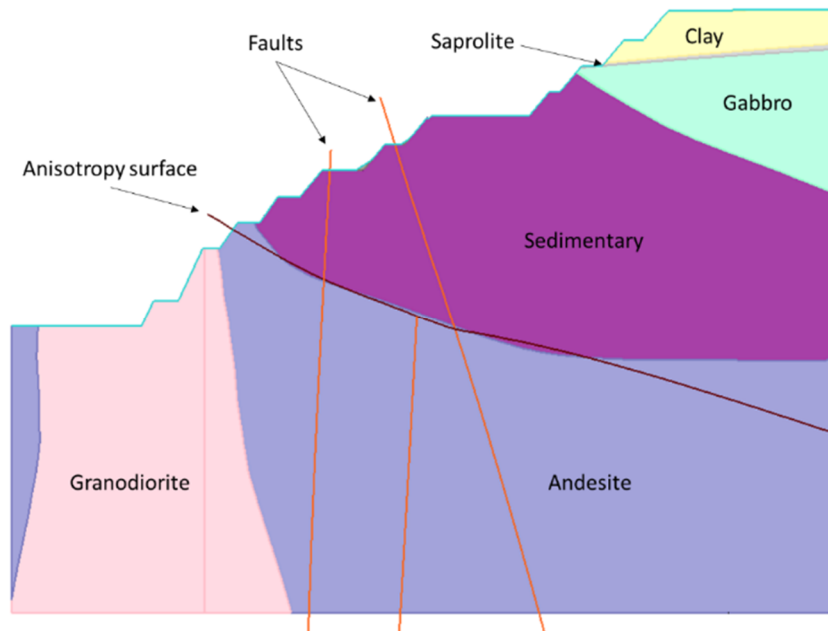


Figure 5 Typical section of geotechnical domains at the south wall (looking east)

Geotechnical data is collected, analysed and regularly revisited in line with the increasing level of understanding mainly based on failure back-analysis and annual geotechnical investigation programs. There are eight different design sectors which cover six planned pit development stages until the end of the life-of-mine (LoM). Current mining is progressing in Stage 2 and the focus of this case study is the south wall, particularly within Sector 6 as shown in Figure 6.

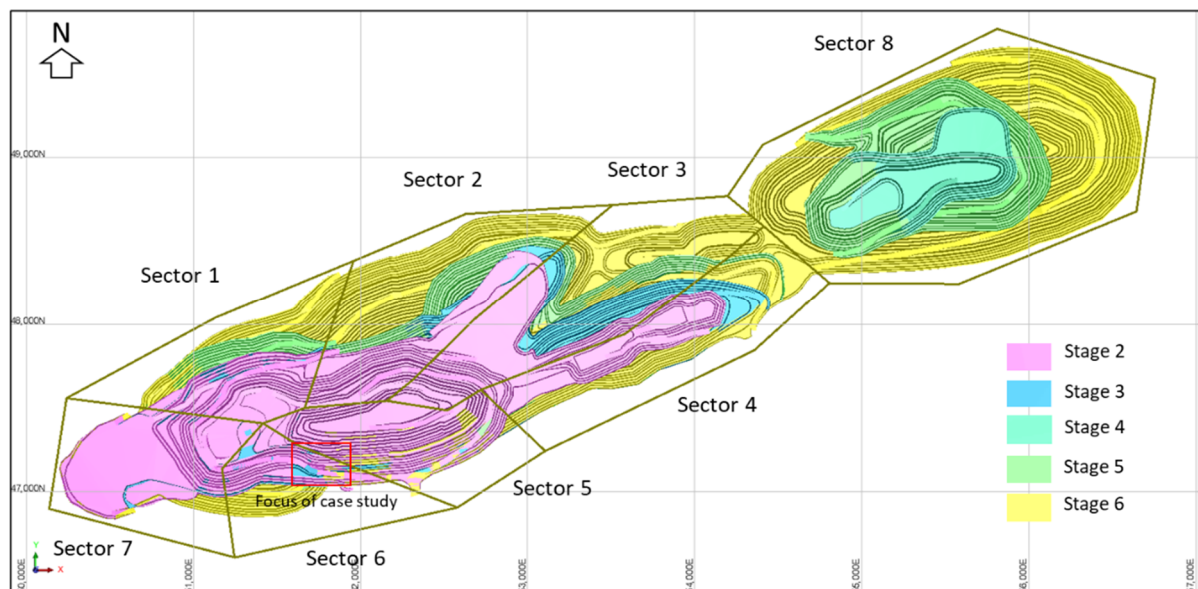


Figure 6 Pit design sectors and development stages with an insert of the case study focus area

The failure mechanisms observed on the south wall in the early mining stages are considered to be complex and, to some degree, uncertain. The weakest part of sedimentary domain is identified by zones of increasing alteration intensity, which causes the material to become locally weaker and more friable within the narrowly

spaced bedding planes. Despite the bedding orientation dipping into the wall and a potential for toppling, field observations so far point to a composite mechanism with rotational failure surface, potentially shearing through the highly altered sediments. The strength of the sedimentary rock mass gradually decreases in the southwest direction while the alteration intensity increases. Ductile ground behaviour is observed in the highly altered sediments and is considered a significant concern for the long-term stability of haulage ramps.

Since the concern with sedimentary domain will also be encountered during future mining stages on the south wall, it is necessary to further investigate it for the purpose of slope optimisation. Within Sector 6, the sedimentary domain has high-intensity hematite alteration and reduced strength compared to the sedimentary domain in another sector, as shown in Figure 7. As a result, the sedimentary domain has been divided into two classes as follows:

- Sedimentary-class 1: high-intensity hematite alteration sedimentary material located at Sector 6. Low-strength anisotropic rock which behaves like soil in some instances. Rotational failure mechanisms observed (Figure 7a).
- Sedimentary-class 2: anisotropic sedimentary material located at Sector 5. Less altered, however, found within a major shear zone within bedded sediments (Figure 7b).

Several disturbed samples in sedimentary-class 1 were also collected and sent to a laboratory for direct shear testing to estimate shear strength parameters, cohesion (c') and the friction angle (ϕ'). Table 1 presents isotropic Hoek–Brown failure criterion material properties derived for rock domains and Mohr–Coulomb material strengths for clays and saprolites. Anisotropic material strength properties are assigned to sedimentary-class 1 and are discussed later, in Section 3. Wall control blasting has been rigorously applied with consideration of a negligible blast disturbance factor ($D = 0$). The geological faults have been (conservatively) assumed as being slickensided or polished planar surface with weak clay infill. Table 1 summarises the adopted geotechnical strength parameters including sedimentary-class 1 in the back-analysis section.

Table 1 Summary of adopted geotechnical shear strength parameters

Domain		Class	Sector	c' kPa	ϕ' °	UCS MPa	GSI	m_i	D	E_i GPa	ν	ϕ	σ_i MPa
Clay			6	22	33								
Saprolite			6	22	39								
Andesite			6			48	60	25	0	41	0.25	0.4	9
Gabbro			6			14	45	15	0	14	0.24	0.5	4
Granodiorite			6			50	65	29	0	26	0.28	0.4	5
Sedimentary	Rock mass	1	6	25	34								
	Bedding	1	6	5	16								
Sedimentary	Rock mass	2	5			48	30	22	0	20	0.26	0.5	6
	Bedding	2	5	5	16								
Faults			All	1	22								

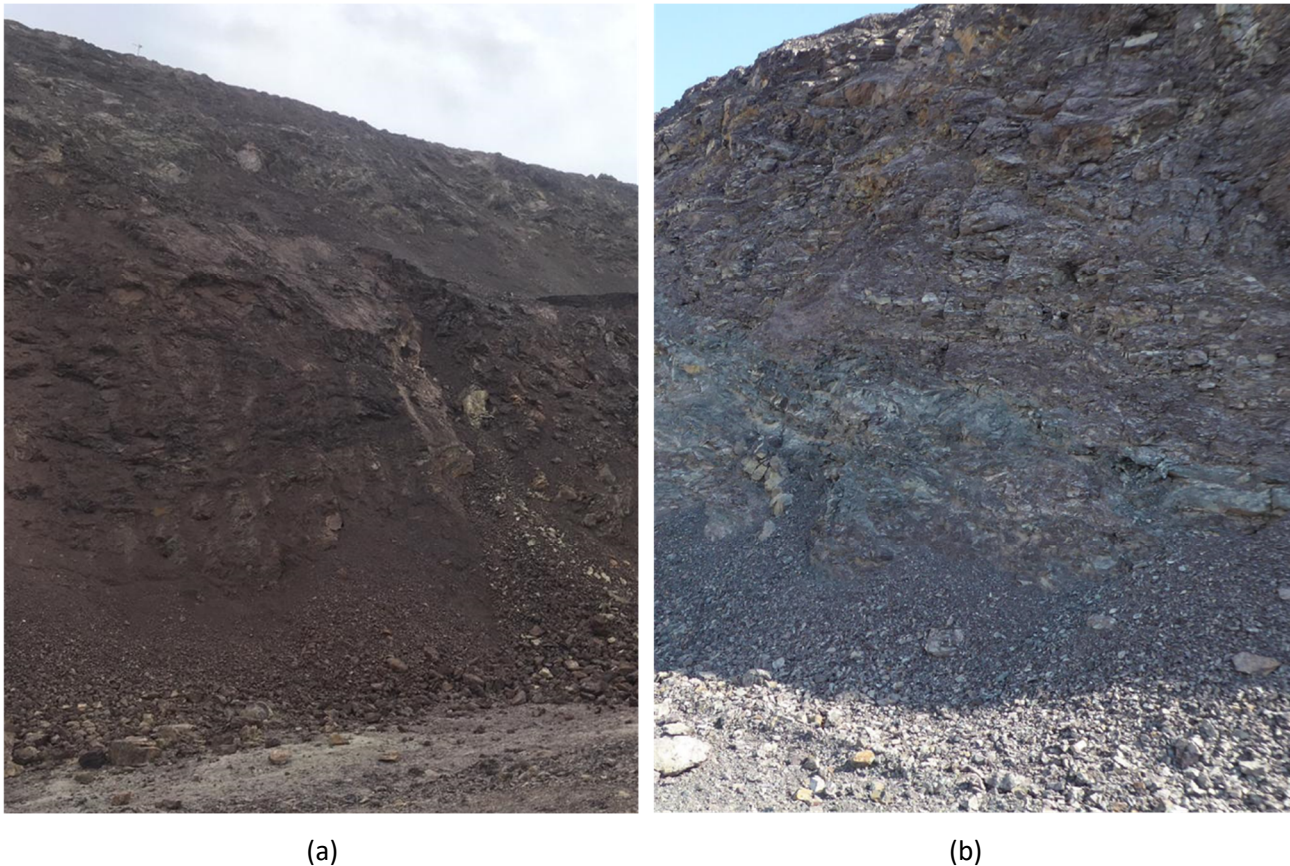


Figure 7 Weaker sedimentary domain with high-intensity hematite alteration at (a) Sector 6 compared to (b) Sector 5

2.3 Groundwater

The groundwater table before mining is situated just a few tens of metres below the surface. In the early mining stages, mine dewatering and slope depressurisation were managed solely through sumps and pumping water from the bottom of the pit and distant bore fields, i.e. no horizontal drilling or in-pit pumping wells were implemented.

The primary source of groundwater information comes from the data obtained via 19 vibrating wire piezometers (VWPs) located around the pit in various inclined boreholes. A basic groundwater modelling method for the purpose of slope stability analysis assigns a phreatic surface below which hydrostatic pore pressures are modified to match field-derived data from VWPs. H_u coefficients are factors between 0 and 1 that are used to correlate real pore pressures (from VWP data) to the model with an assigned phreatic surface. H_u coefficient values are derived to calculate pore pressure in a slope stability model as follows:

- $H_u = 0$ would indicate a dry soil or rock mass. Pore pressure will be zero.
- $H_u = 1$ would indicate fully saturated, hydrostatic conditions.
- $H_u > 1$ would indicate pore pressures higher than hydrostatic conditions (e.g. high pressure in an artesian aquifer).

H_u coefficients derived in this case study are based on the assignment of a phreatic surface that follows the topographic surface. This phreatic surface has been assumed for the following reasons:

- The high regional groundwater table is able to reflect the current mine dewatering practices.
- Pore pressure management strategies are not yet defined in the mine closure plans.
- It provides flexibility for assessing multiple mine designs and groundwater sensitivities.

Piezometric pressure (m of head) for each VWP is compared against the depth of the VWP sensor below the topographic or ground surface (see Figure 8). An H_u coefficient of 0.75 is applicable when considering all available data from the spring season during the snowmelt period where geotechnical risks associated with pore pressures are at their highest.

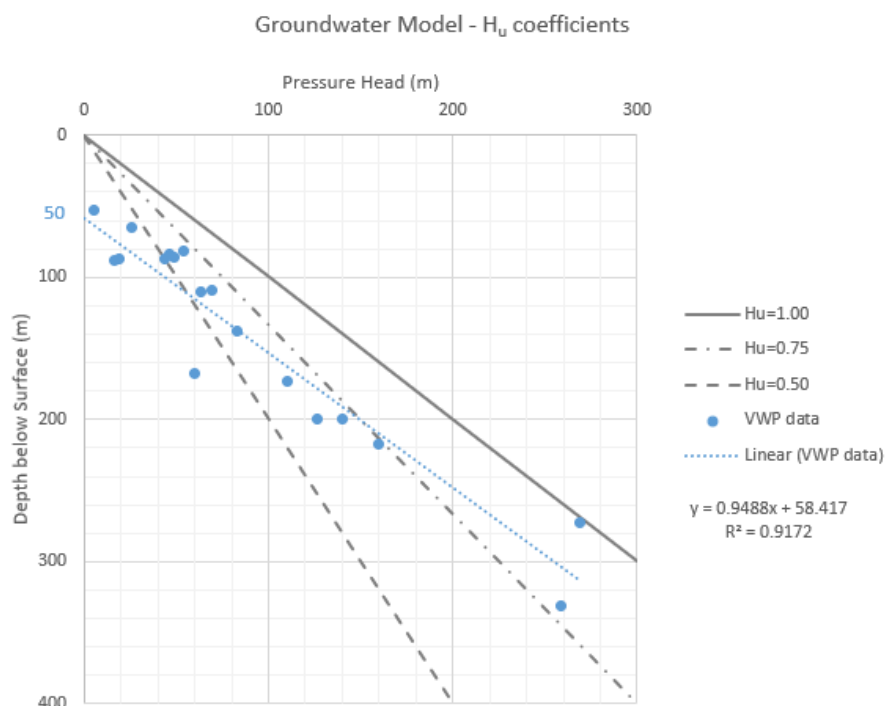


Figure 8 VWP data from spring 2022 used to derive groundwater model H_u coefficients

Based on Figure 8, the top 50 m of ground beneath the surface in proximity to the pit, which mainly consists of clay and saprolite domains, is considered dry with $H_u = 0.00$.

3 Three-dimensional back-analysis

To ensure the design of reliable and stable slopes it is crucial that the model accurately represents the actual geological conditions and is considered as representative. The material geometry for the 3D slope stability model in this case is constructed referring to the available solid wireframes. The lower contact of sedimentary domain is assigned as an anisotropy plane surface and has been validated in several locations through core logging and photogrammetry.

Back-analysis focuses on the instability area within the sedimentary domain to refine material properties. 3D limit equilibrium software *Slide3* from RocScience Inc was utilised for the back-analysis. Qualitative model validation is carried out by comparing the modelled failure surface with a deformation map from slope stability monitoring radar to facilitate spatial and material property validation:

- Spatial validation: the unconstrained model replicates the correct failure location and shape.
- Material property validation: the material properties used attain a Factor of Safety (FoS) = 1.00 ± 0.02 .

The following considerations were made to develop the model and complete the back-analysis in several iterative steps:

- *Slide3* failure back-analysis:
 - Analysis used a general limit equilibrium method of columns. Additional checks were completed using Bishop's Method and Janbu's Method of columns.

- A generalised anisotropic strength model was applied to the sediments domain with the bedding strength following an anisotropy surface defined by the basal contact of the sediments. Generalised anisotropic variability parameters $A = 15^\circ$ and $B = 30^\circ$ were adopted, based on previous work in sedimentary rock masses by Bar & Weekes (2017). Variability parameter, A , is selected, in part, to the resolution of 3D slip surfaces in limit equilibrium analysis software (Bar & McQuillan 2018): that is, higher variability is needed for the generation of 3D slip surfaces compared to 2D polylines.
- Isotropic material strength properties from Table 1 were applied to the remainder of the soil and rock masses.
- Known geological faults as weak layers (i.e. interfaces) were included in the model.
- The groundwater table followed the external surface with customising H_u coefficients. Sensitivity analysis for the potential variation of pore pressures using H_u coefficients was also completed.
- Probabilistic input parameters were used in *Slide3* along with the particle swarm method for slip surface generation, with additional surface altering optimisation to find a range of plausible material strengths that result in equilibrium conditions.
- Spatial validation with IBIS ArcSAR radar data:
 - The influence of faults in the stability model were assessed. Most were sub-vertical and had negligible influence on the model outputs.
 - The model output was visually compared against the actual displacement data.
 - Model inputs and re-run models were adjusted as appropriate until a spatial match was achieved.

The original slope component parameter for strongly altered sedimentary domain at Sector 6 comprises 55° bench face (batter) angle, 10 m-high benches and 7.5 m-wide benches (berms), with a resultant inter-ramp angle (IRA) of 34.6° . This geometry formed the basis of the pre-failure conditions in Stage 2.

The probabilistic analysis was performed to assess the correlation of cohesion and friction angles that meet FoS as close to 1.0 ($FoS \approx 1.0$) as practicable. Initial values for bedding strength are based on mean average laboratory data with a plausible range in cohesion of ± 6 kPa and a friction angle of $\pm 6^\circ$.

Displacements within the sediments were correlated with potential changes in pore pressure from rainfall and during the snowmelt. Groundwater is modelled as previously discussed with the use of H_u coefficients. However, to better understand groundwater sensitivity and respective strength parameters, three groundwater scenarios were tested:

- $H_u = 1.00$: assumption of fully saturated conditions, although considered very pessimistic.
- $H_u = 0.75$: based on the available VWP data.
- $H_u = 0.00$: assumption of fully depressurised conditions, although considered very optimistic.

Figure 9 illustrates the correlation of back-analysed rock mass cohesion and friction angle. In this case, a good spatial correlation and strength parameter correlation with $FoS \approx 1$ was achieved.

RocScience *Slide3* software was able to model back-analysis with failure surface contour reflecting the area of cracks and settlement at the upper bench adjacent to the main haulage ramp. The back-analysis result provides the material strength properties for sedimentary-class 1:

- Rock mass strength: cohesion of 25 kPa and friction angle of 34° .
- Bedding strength: cohesion of 5 kPa and friction angle of 16° .
- The back-analysis output in *Slide3* is presented in Figure 10.



SSIM 2023, Perth, Australia

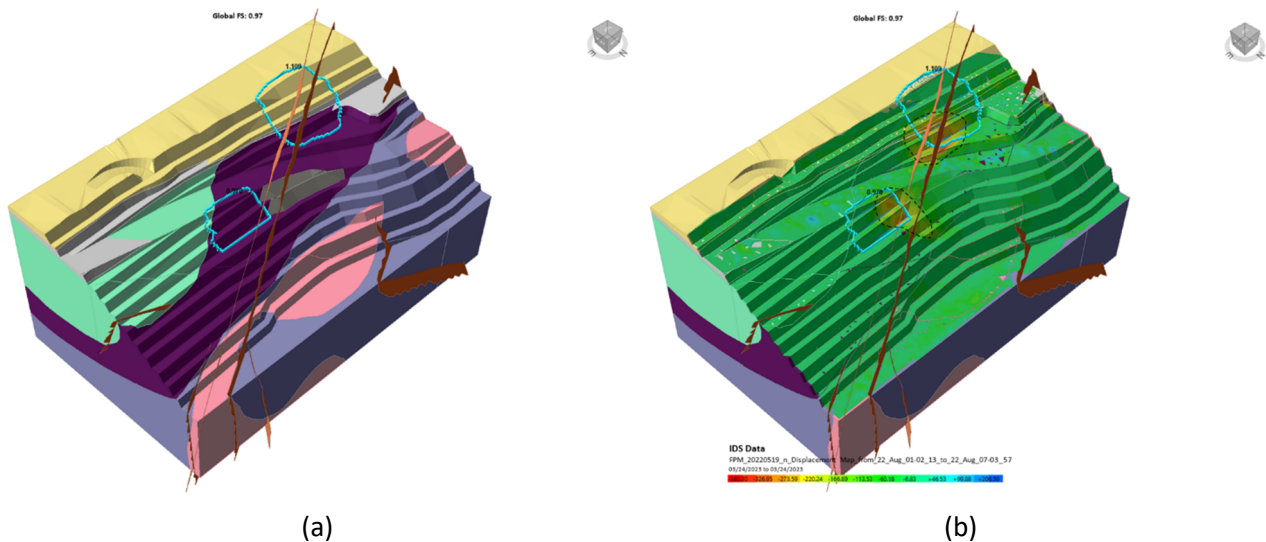


Figure 11 (a) Validation result in *Slide3* with multiple failure surface search (b) overlaid with deformation contour from slope stability radar monitoring

4 Three-dimensional forward analysis

Forward analysis was subsequently performed for proposing stable slope design configuration. In addition to 3D limit equilibrium, 3D software *RS3* from RocScience Inc was used for validation and to investigate the potential for a complex failure mechanism. Within the sediments domains, adopted shear strength parameters from Table 1 were used for the base case modelling which needed to meet the design acceptance criteria (DAC) in Table 3. Back-analysed shear strength parameters for sedimentary-class 1 were used for sensitivity analyses, which need to meet a lower minimum FoS in the DAC (Table 3).

The objective for the future Stage 3 pushback was to achieve long-term stable and reliable slope designs that require minimum maintenance. Improving bench scale stability was a primary driver, and reduced BFA resulted in also reducing the IRA as shown in Table 2. Forward analysis was completed using similar considerations to the back-analysis and three pore pressure scenarios using H_u coefficients to simulate future slope depressurisation targets, and their effect on stability.

Due to the larger spatial extent of the forward analysis for the future Stage 3 pushback, the model geometry was updated as shown in Figure 12, which illustrates the constrained model boundary of Stage 3 pushback design.

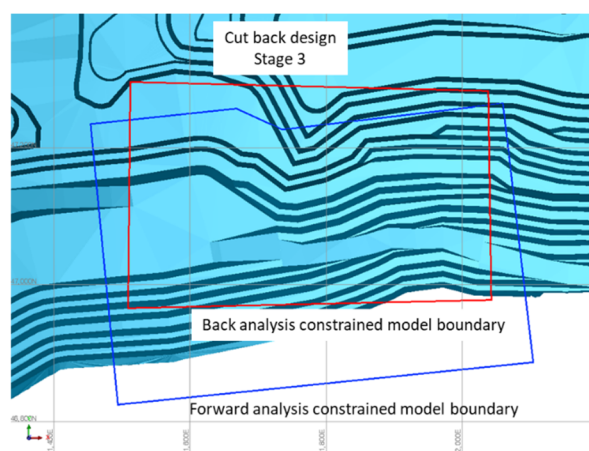


Figure 12 Constrained model boundary with respect to external surface of Stage 3 pushback design

Table 2 Slope component parameter comparison

Domain	Design	Batter angle (°)	Bench height (m)	Berm width (m)	Inter-ramp angle (°)
Sedimentary-class 1	Stage 2	55	10	7.5	35 (34.6)
	Stage 3 pushback	45	10	7.5	30 (29.7)

Within the same model, variations of $H_u = 0.75$, $H_u = 0.60$ and $H_u = 0.50$ were assessed to investigate the influence of the groundwater table with respect to the DAC. The base case model uses $H_u = 0.75$, which assumes that the future Stage 3 pushback implements the slope geometry adjustment only, without any slope depressurisation effort (i.e. no horizontal drilling or additional pumping wells). Conversely, $H_u = 0.60$ and $H_u = 0.50$ further assess for groundwater sensitivity on slope stability with the premise to set up depressurisation targets to improve FoS. For an inter-ramp slope with a moderate consequence of failure, the DAC requires a minimum FoS = 1.2 for the base case. The DAC presented in Table 3 is based on suggested values from Read & Stacey (2009) but has been adjusted to consider the static base case and sensitivity analyses which can include pseudo-static analysis, lower-bound strengths, increased pore pressure due to snowmelt or high-intensity rainfall etc.

Table 3 Typical FoS and Probability of Failure (PoF) design acceptance criteria values

Slope scale	Consequences of failure	Design acceptance criteria		
		FoS (min) (base case)	FoS (min) (sensitivity)	PoF (max) P[FoS ≤ 1]
Bench	Low-high	1.1	NA	25–50%
Inter-ramp	Low	1.15–1.2	1.0	25%
	Moderate	1.2	1.0	20%
	High	1.2–1.3	1.1	10%
Overall	Low	1.2–1.3	1.0	15–20%
	Moderate	1.3	1.05	10%
	High	1.3–1.5	1.1	5%

Faults as weak planes are modelled as suppressed and unsuppressed to figure out their influence on stability and investigate whether any potential failure could be controlled by structures. FoS for each H_u scenario are obtained for each suppressed and unsuppressed faults model by using RocScience *Slide3* software. Figure 13 and Table 4 summarise FoS results for each scenario. Effectively, the sub-vertical geological faults have negligible impact on slope stability. Slope depressurisation has the potential to significantly improve FoS.

Table 4 FoS summary table for forward analysis of each depressurisation scenario

H_u	FoS: suppressed faults	FoS: unsuppressed faults	Remarks
0.75	1.14	1.14	Marginal stability
0.60	1.28	1.26	Achieved static acceptance criteria
0.50	1.37	1.33	Achieved static acceptance criteria

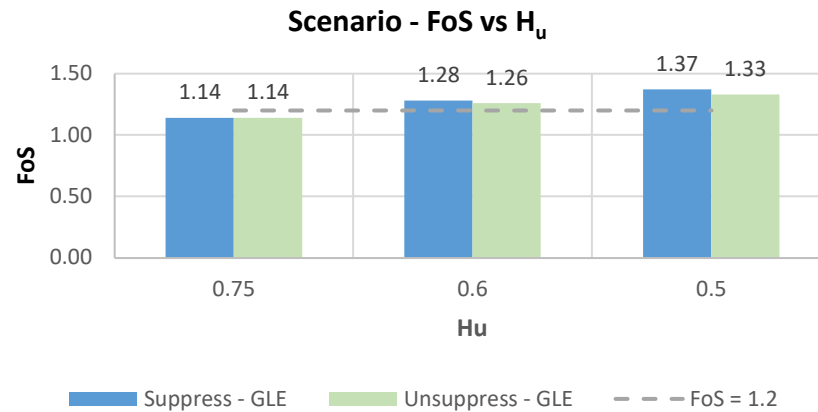


Figure 13 FoS summary chart for forward analysis of each depressurisation scenario

Elastic analysis in 3D software RocScience *RS3* validates the *Slide3* result. Total displacement and maximum shear strain are displayed, including cross-sections at the highest values to visualise contours behind the external surface. No additional complex failure mechanisms were identified using finite element analysis. Figure 14 presents the 3D limit equilibrium and elastic finite element model results for Stage 3.

As part of a LoM study, additional modelling was completed on a full pit scale using the 3D limit equilibrium method. This study investigated stability for Stage 3 and beyond with the aim of understanding potential inter-ramp and overall slope scale risks and opportunities associated with rock mass failure modes and structurally driven failure modes.

Analysis methods were similar to the back-analysis discussed earlier. However, all slip surfaces were bounded to have a minimum slip surface at a depth of 30 m below the external boundary to avoid analysing for local and operationally manageable bench instabilities. A total of 45 discrete geological faults were included in the full pit scale model.

Ellipsoidal slip surfaces were generated using:

- A particle swarm search for assessing multiple low FoS slip surfaces comprising both rock mass failure and structurally driven failure modes.
- A cuckoo search for 10 overlapping spatial domains for assessing the lowest FoS slip surface within each domain comprising both rock mass failure and structurally driven failure modes.

All slip surface were subsequently optimised using surface alteration algorithms to find the lowest FoS. Faults were included as weak layers that intersect the rock mass and pit slope geometry at various locations and orientations.

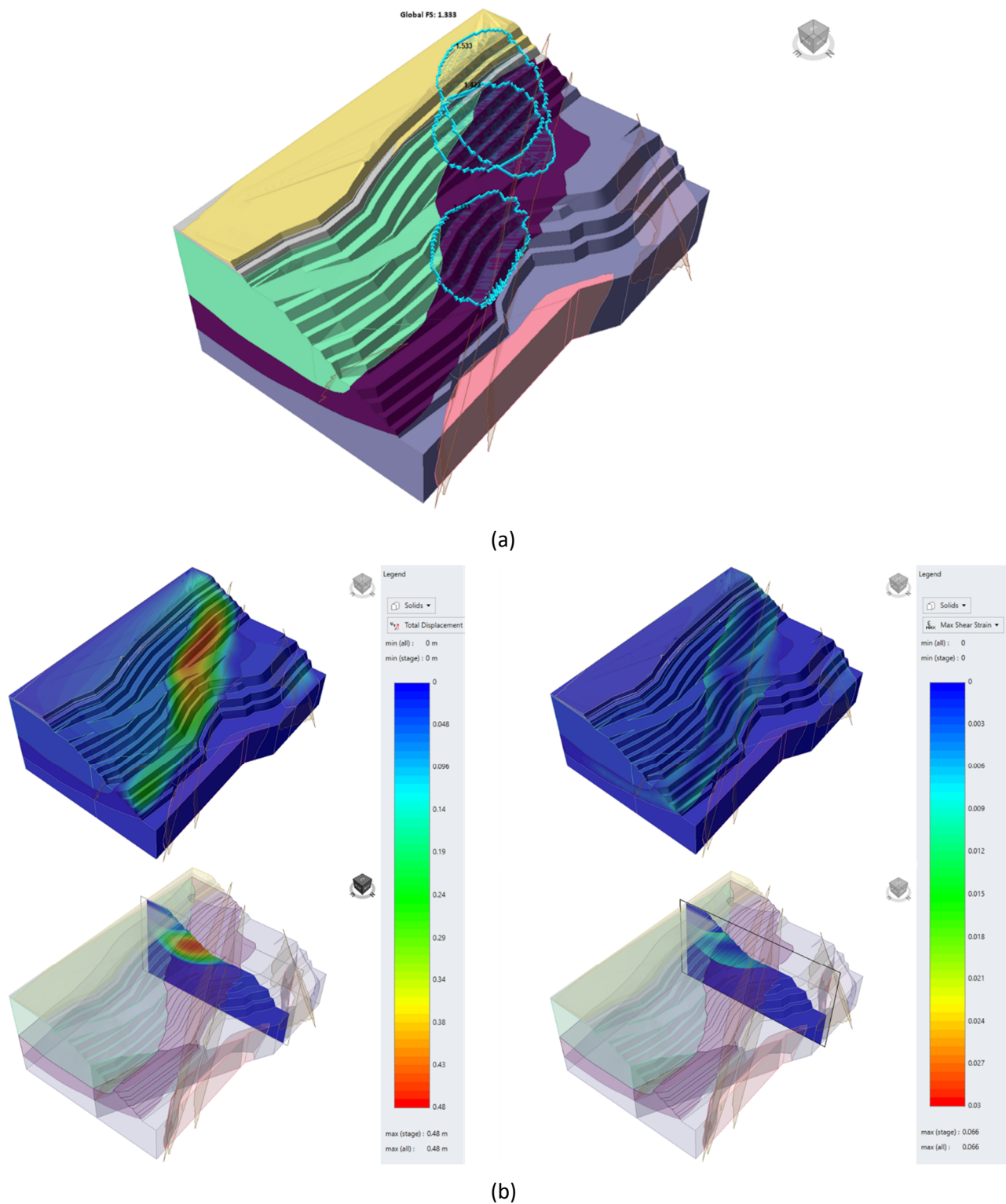
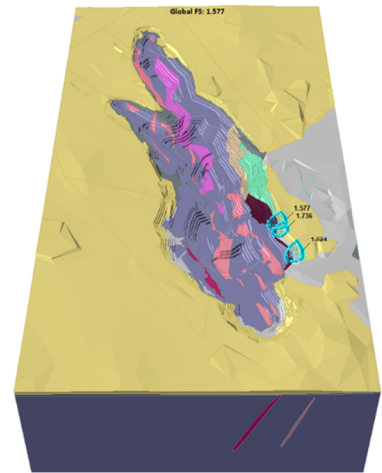
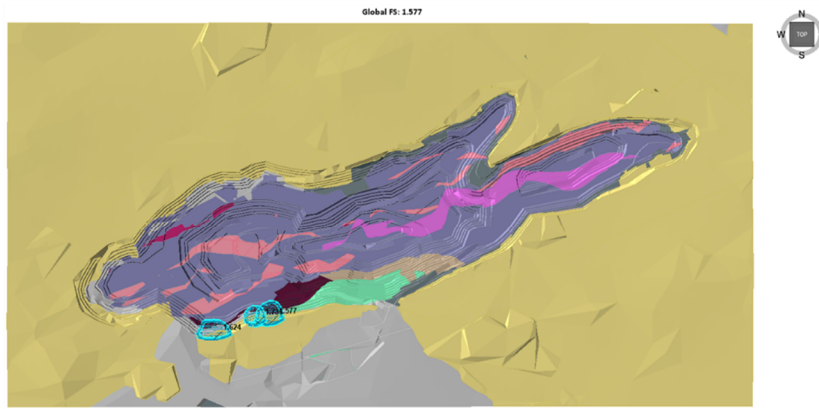
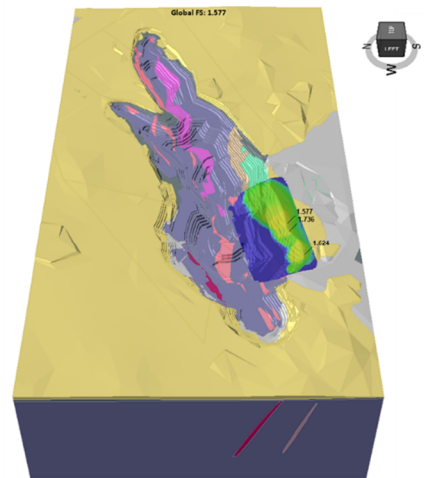
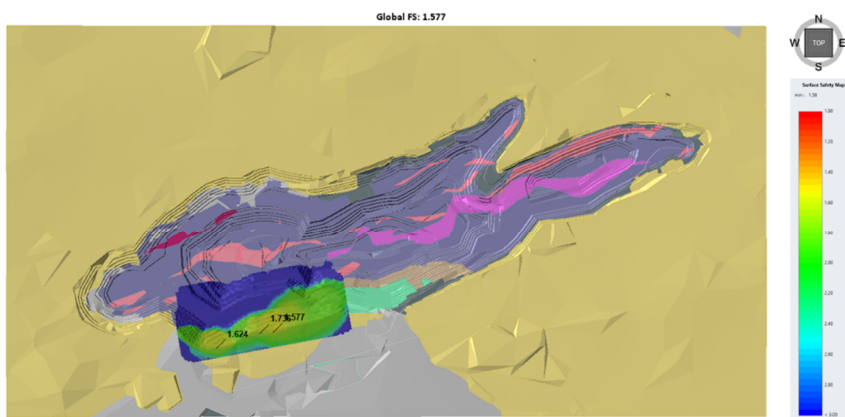


Figure 14 (a) Forward analysis result in *Slide3*; (b) With validation result in *RS3* (e.g. for $H_u = 0.5$)

Figures 15 and 16 show the analysis results for the same slope sector previously reviewed in the back-analysis. The results indicated the FoS exceeds DAC for both the particle swarm search and cuckoo search ($FoS > 1.2$) for inter-ramp slopes, signifying a low-risk design and potential opportunities for slope optimisation.

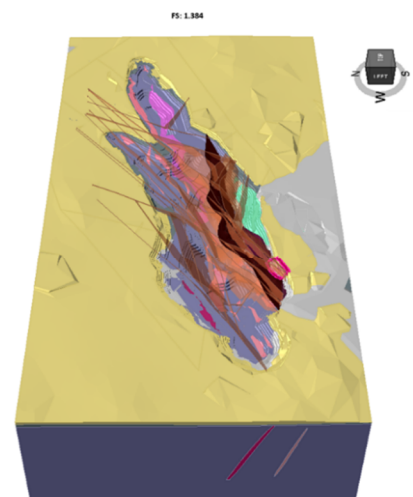
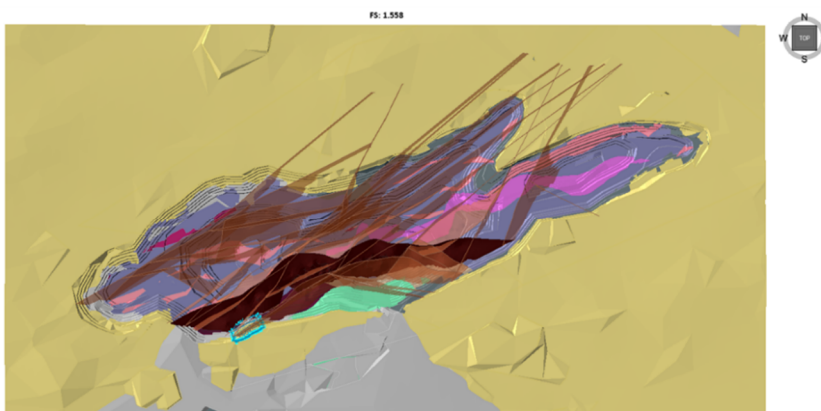


(a)



(b)

Figure 15 *Slide3* output for full pit scale to assess rock mass failure modes by using particle swarm presenting (a) multiple failure surfaces and (b) a FoS heat map



(a)

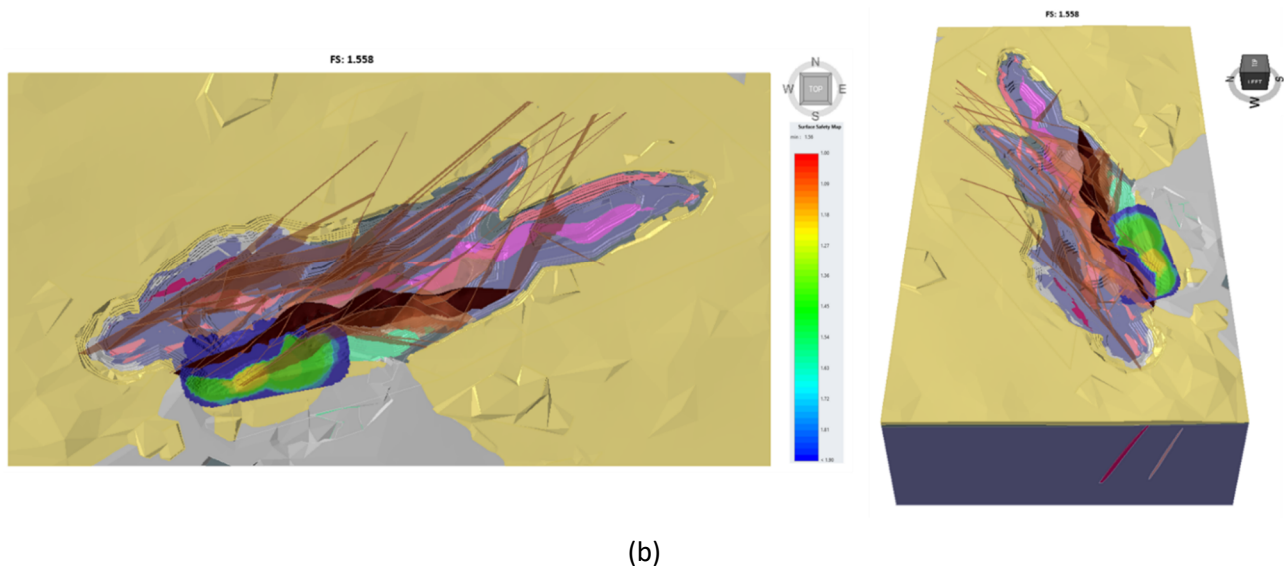


Figure 16 *Slide3* output for full pit scale to assess structurally driven failure modes by using a cuckoo search presenting (a) a global minimum failure surface and (b) a FoS heat map

5 Conclusion

Based on the back-analysis results and subsequent forward analysis on local and global models, the following recommendations were proposed to improve slope stability for further Stage 3 pushback design and LoM mine plans:

- Within the sediments-class 1 domain, reducing the IRA to 29.7° (from 34.6°) by implementing 45° bench face angles, 10 m bench height and 7.5 m berm width for long-term stability.
- Improving the stability by reducing porewater pressure. This requires a high-density network of VWP's and the commencement of horizontal drilling to depressurise the south wall slopes.
- Adding geotechnical site investigations including additional diamond drilling and borehole geophysics to further refine geomechanical understanding of the sediments domain.

The challenging slope stability conditions at Bozshakol pit south wall, particularly on a strongly altered sedimentary domain, have been safety and economically managed through a comprehensive monitoring and response processes and ongoing remedial works.

In this study, the south wall instabilities have been back-analysed to refine material properties for a more reliable future prediction, which has resulted in a minor slope design change for the upcoming Stage 3 pushback. It has also demonstrated the need for slope depressurisation and helps to demonstrate the economic value of horizontal drilling.

The use of 3D limit equilibrium analysis has been integrated into the geotechnical workflow and is now used as part of annual LoM design reviews and for slope reconciliation processes.

Acknowledgement

The authors would like to acknowledge the support from KAZ Minerals Bozshakol colleagues, particularly mine engineering and mine operations personnel, for their ongoing efforts in managing geotechnical risks. Permission from KAZ Minerals to publish this paper is highly appreciated.

References

- AMC Consultants Pty Ltd 2010, *Bozshakol Feasibility Study – Geotechnical*, unpublished report, AMC Consultants Pty Ltd, Melbourne.
- Bar, N & Weekes, G 2017, 'Directional shear strength models in 2D and 3D limit equilibrium analyses to assess the stability of anisotropic rock slopes in the Pilbara region of Western Australia', *Australian Geomechanics Journal*, vol. 52, no. 4, pp. 91–104.
- Bar, N & McQuillan, A 2018, '3D limit equilibrium slope stability analysis for anisotropic and faulted rock masses in Australian coal and iron ore mines', *ISRM International Symposium - 10th Asian Rock Mechanics Symposium*, OnePetro, Singapore, pp. 12.
- KAZ Minerals 2023, *Bozshakol*, viewed 17 October 2023, www.kazminerals.com/our-business/bozshakol
- Read, J & Stacey, P 2009, *Guidelines for Open Pit Slope Design*, CSIRO Publishing, Melbourne.
- Shen, P, Pan, H, Seitmuratova, E, Yuan, F & Jakupova, S 2015, 'A Cambrian intra-oceanic subduction system in the Bozshakol area, Kazakhstan', *Lithos*, vol. 224–225, pp. 61–77.
- Tektonik 2022, *Bozshakol Cu Deposit, Kazakhstan: Structural Geological Model to Support Geotechnical and Hydrogeological Planning*, unpublished report, Tektonik Consulting Limited, South Wales.

